ELSEVIER

Chemical Engineering Journal 135 (2008) 157–167

Chemical Engineering Journal

www.elsevier.com/locate/cej

Review

Kinetics and kinematics for the metal oxidation on a spherical geometry

Eun-Suok Oh *

LG Chem/Research Park, 104-1 Moonji-dong, Yuseong-gu, Daejeon 305-860, Republic of Korea

Received 21 July 2006; received in revised form 10 March 2007; accepted 13 March 2007

Abstract

The oxidation of a metal sphere is analyzed using a regular perturbation method and an inelastic approach. As shown in our previous work [E.-S. Oh, A diffusional analysis for the oxidation on a plane metal–oxide interface, Chem. Eng. J. 117 (2006) 143–154; E.-S. Oh, A perturbation analysis for the metal oxidation fo cylindrical geometries, J. Chem. Eng. Japan 39 (1) (2006) 57–67], the perturbation analysis provides detailed information on the oxide thickness from the location of both moving metal–oxide and oxide–oxygen (air) interfaces, as well as on the concentration of oxygen in each phase. This is compared to the result numerically calculated in literature [P.B. Entchev, D.C. Lagoudas, J.C. Slattery, Effects of non-planar geometries and volumetric expansion in the modeling of oxidation in titanium, Int. J. Eng. Sci. 39 (2001) 695–714]. In addition, a simple inelastic approach [E.-S. Oh, J.R. Walton, D.C. Lagoudas, J.C. Slattery, Evolution of stresses in a simple class of oxidation problems, Acta Mech. 181 (2006) 231–255] is applied to calculate the stress distribution developed during the oxidation of the metal sphere.

Keywords: Diffusion; Oxidation; Perturbation analysis; Landau transformation; Stress distribution

1. Introduction

Over the past half of a century a great number of research work on the oxidation of metal has been published in open literature. Especially, the reaction kinetics including the mechanism of oxide growth on a flat surface has been extensively studied and considerable progress has been made in the field. While much less attention has been paid to the metal oxidation of non-planar geometries. In more recent years, some studies on the oxidation of non-planar metals have been motivated due to the development of non-planar VLSI devices [5,6], and the degradation of metal matrix composites [7,8] and metallic particles [9,10]. However, no exact solutions on the oxide growth have been available for the metal oxidation of non-planar geometries. There are a few analytical and numerical solutions available under some assumptions such as no oxygen diffusion into metal, no volumetric expansion, and a diffusion-controlled oxidation [3,7,11,12].

In our previous works [1,2], we obtained expressions for the oxide growth on both flat and cylindrical geometries without using typical assumptions mentioned above. A regular perturbation analysis with the Landau transformation [13] was employed. In this paper, we will again use the perturbation analysis to solve the spherical oxidation problem. This will be compared to the result numerically calculated by Entchev et al. [3] for a special case of titanium oxidation.

Additionally, we will calculate the stress developed during the spherical oxidation. Typically, the density of the oxide formed at the metal–oxide interface is different from that of the metal consumed at the interface. This results in volumetric expansion or contraction and thus stresses develop in both the metal and the oxide as oxidation proceeds. The inelastic approach first employed for cylindrical systems by Oh et al. [4] will be extended to the spherical oxidation to calculate the stresses. By the inelastic approach, we mean that unlike most elasticity problems, the oxidation problem will be handled with the current configuration known by the above perturbation analysis.

* Tel.: +82 42 870 6076; fax: +82 42 862 6072.
E-mail address: eunsuokoh@gmail.com.

1385-8947/$ – see front matter © 2007 Elsevier B.V. All rights reserved.
doi:10.1016/j.cej.2007.03.021

Nomenclature

$c_{(A)}^{(B)}$	concentration of A in phase B
c_{eq}	equilibrium concentration of oxygen at the oxide–oxygen (air) interface
$\mathcal{D}^{(B)}$	diffusion coefficient of oxygen in phase B
$E^{(B)}$	Young's modulus in phase B
$\mathbf{I}$	identity tensor
k	reaction rate coefficient for the oxidation
$\mathbf{N}_{O_2}^{(B)}$	molar flux of oxygen in phase B
$r_{(A)}^{(\sigma)}$	rate of production of species A at the metal–oxide interface
R_{ini}	initial radius
R_i	inner radius
R_o	outer radius
s	surface whose concentration of oxygen is assumed to keep the initial state
$\mathbf{u}$	displacement vector
$v_{(A)}^{(B)}$	velocity of A in phase B

Greek letters

α	ratio of the diffusion coefficient of oxygen in metal to that in oxide
χ_o	ratio of R_o to R_i
χ, ζ	variables for new coordinate systems
$\boldsymbol{\varepsilon}$	strain tensor
ϕ	perturbation parameter
γ	Pilling-Bedworth ratio
$\nu^{(B)}$	Poisson's ratio in phase B
$\boldsymbol{\sigma}$	Cauchy stress tensor

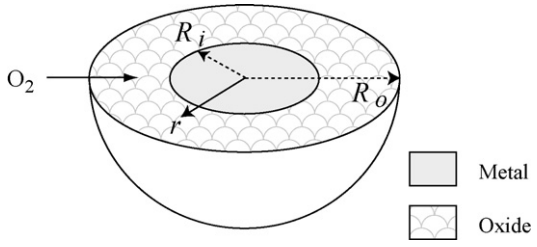

Fig. 1. The oxidation of a metal sphere.

2. Problem statement

As shown in Fig. 1, a solid sphere initially composed of pure metal is exposed to oxygen environment. Both R_i and R_o are functions of time, and initially $R_i(0) = R_o(0) = R_{ini}$, where R_{ini} is the initial radius of the sphere. The following assumptions will be made to model the oxidation of the metal sphere:

(i) The frame of reference is chosen such that the metal is stationary.
(ii) The metal is initially oxygen-free.
(iii) Equilibrium is established at the oxide–oxygen (air) interface.
(iv) The molar density of metal $c_{(met)}$ and the molar density of oxide $c_{(ox)}$ are independent of position and time.
(v) Temperature is independent of position and time, which means that the energy released by the reaction is dissipated rapidly.
(vi) Oxygen diffuses through the oxide to react with the metal to form fresh oxide at the metal–oxide interface. The oxidation is a simple first-order reaction with respect to oxygen.
(vii) The materials are assumed to be isotropic linear elastic solids described by the generalized Hooke's law

$$\boldsymbol{\sigma} = \frac{E}{1+\nu}\left(\boldsymbol{\varepsilon} + \frac{\nu}{1-2\nu}\,\mathrm{tr}\,\boldsymbol{\varepsilon}\,\mathbf{I}\right) \tag{1}$$

where $\boldsymbol{\sigma}$ is the Cauchy stress tensor, $\boldsymbol{\varepsilon}$ is the strain tensor

$$\boldsymbol{\varepsilon} = \tfrac{1}{2}(\nabla\mathbf{u} + \nabla\mathbf{u}^{\mathrm{T}}) \tag{2}$$

where $\mathbf{u}$ is the displacement vector with respect to the appropriate reference configuration, and E and ν are, respectively, the Young's modulus and the Poisson's ratio of the material.

(viii) All physical parameters are considered to be constants.

3. Oxidation of a metal sphere

Oxygen diffuses through the oxide to react with the metal to form fresh oxide at the metal–oxide interface:

$$a\,\mathrm{Metal} + \mathrm{O_2} \rightarrow b\,\mathrm{Oxide} \tag{3}$$

In view of assumption (vi), we have

$$r^{(\sigma)}_{(\mathrm{O_2})} = \frac{r^{(\sigma)}_{(\mathrm{met})}}{a} = -\frac{r^{(\sigma)}_{(\mathrm{ox})}}{b} = -k\,c^{(\mathrm{o})}_{(\mathrm{O_2})} \tag{4}$$

where $r^{(\sigma)}_{(A)}$ is the rate of production of species A per unit area on the metal–oxide interface and k is a reaction constant for the oxidation.

The differential mass balances [14] for $\mathrm{O_2}$ in the metal and its oxide layer are

$$\frac{\partial c^{(\mathrm{m})}_{(\mathrm{O_2})}}{\partial t} = \frac{\mathcal{D}^{(\mathrm{m})}}{r^2}\frac{\partial}{\partial r}\left(r^2\frac{\partial c^{(\mathrm{m})}_{(\mathrm{O_2})}}{\partial r}\right) \tag{5}$$

$$\frac{\partial c^{(\mathrm{o})}_{(\mathrm{O_2})}}{\partial t} + v^{(\mathrm{o})}_{(\mathrm{ox})}\frac{\partial c^{(\mathrm{o})}_{(\mathrm{O_2})}}{\partial r} = \frac{\mathcal{D}^{(\mathrm{o})}}{r^2}\frac{\partial}{\partial r}\left(r^2\frac{\partial c^{(\mathrm{o})}_{(\mathrm{O_2})}}{\partial r}\right) \tag{6}$$

where superscripts m and o refer to the metal and oxide layers. $c_{(\mathrm{O_2})}$, $v_{(\mathrm{ox})}$, and $\mathcal{D}$ are the molar concentration of oxygen, the velocity of oxide and the diffusion coefficient of oxygen, respectively. Note that the velocity of the oxide in the oxide layer $v^{(\mathrm{o})}_{(\mathrm{ox})}$ is not zero if there exists the density difference between the metal and its oxide [2].

Using the jump momentum balances at both interfaces, Fick's first law, and the differential mass balance for oxide, as given in our previous papers [1,2,4], we finally have

$$v^{(\mathrm{o})}_{(\mathrm{ox})}(r,t) = \frac{a - b\gamma}{c^{(\mathrm{m})}_{(\mathrm{met})}\epsilon}\left(\frac{R_{\mathrm{i}}}{r}\right)^2\left(\mathcal{D}^{(\mathrm{m})}\frac{\partial c^{(\mathrm{m})}_{(\mathrm{O_2})}}{\partial r}\bigg|_{R_{\mathrm{i}}} - \mathcal{D}^{(\mathrm{o})}\frac{\partial c^{(\mathrm{o})}_{(\mathrm{O_2})}}{\partial r}\bigg|_{R_{\mathrm{i}}}\right) \tag{7}$$

for the spherical system shown in Fig. 1. Here, we have introduced

$$\gamma \equiv \frac{c^{(\mathrm{m})}_{(\mathrm{met})}}{c^{(\mathrm{o})}_{(\mathrm{ox})}}, \quad \epsilon \equiv 1 + \frac{b\,\gamma c^{(\mathrm{o})}_{(\mathrm{O_2})}|_{R_{\mathrm{i}}} - a\,c^{(\mathrm{m})}_{(\mathrm{O_2})}|_{R_{\mathrm{i}}}}{c^{(\mathrm{m})}_{(\mathrm{met})}} \tag{8}$$

This allows Eqs. (5) and (6) to take the forms

$$\frac{\partial c^{(\mathrm{m})}_{(\mathrm{O_2})}}{\partial t} - \frac{2\mathcal{D}^{(\mathrm{m})}}{r}\frac{\partial c^{(\mathrm{m})}_{(\mathrm{O_2})}}{\partial r} - \mathcal{D}^{(\mathrm{m})}\frac{\partial^2 c^{(\mathrm{m})}_{(\mathrm{O_2})}}{\partial r^2} = 0 \tag{9}$$

$$\frac{\partial c^{(\mathrm{o})}_{(\mathrm{O_2})}}{\partial t} - \mathcal{D}^{(\mathrm{o})}\left\{\frac{2}{r} - \frac{a - b\,\gamma}{c^{(\mathrm{m})}_{(\mathrm{met})}\epsilon}\left(\frac{R_{\mathrm{i}}}{r}\right)^2\left[\alpha\frac{\partial c^{(\mathrm{m})}_{(\mathrm{O_2})}}{\partial r}\bigg|_{R_{\mathrm{i}}} - \frac{\partial c^{(\mathrm{o})}_{(\mathrm{O_2})}}{\partial r}\bigg|_{R_{\mathrm{i}}}\right]\right\}\frac{\partial c^{(\mathrm{o})}_{(\mathrm{O_2})}}{\partial r} - \mathcal{D}^{(\mathrm{o})}\frac{\partial^2 c^{(\mathrm{o})}_{(\mathrm{O_2})}}{\partial r^2} = 0 \tag{10}$$

where

$$\alpha \equiv \frac{\mathcal{D}^{(\mathrm{m})}}{\mathcal{D}^{(\mathrm{o})}} \tag{11}$$

In view of assumption (ii), the initial condition is

$$\text{at } t = 0: \; c^{(\mathrm{m})}_{(\mathrm{O_2})}(r,t) = 0 \tag{12}$$

Eqs. (9) and (10) are to be solved consistent with the following boundary conditions [2]:

$$\text{as } r \to s: \; c^{(\mathrm{m})}_{(\mathrm{O}_2)} \to 0 \tag{13}$$

$$\text{at } r = R_\mathrm{o}: \; c^{(\mathrm{o})}_{(\mathrm{O}_2)} = c_\mathrm{eq} \tag{14}$$

$$\text{at } r = R_\mathrm{i}: \; \mathcal{D}^{(\mathrm{o})} \frac{\partial c^{(\mathrm{o})}_{(\mathrm{O}_2)}}{\partial r} - \mathcal{D}^{(\mathrm{m})} \frac{\partial c^{(\mathrm{m})}_{(\mathrm{O}_2)}}{\partial r} = k\epsilon\, c^{(\mathrm{o})}_{(\mathrm{O}_2)} \tag{15}$$

$$\text{at } r = R_\mathrm{i}: \; c^{(\mathrm{m})}_{(\mathrm{O}_2)} = c_\mathrm{s} \tag{16}$$

Here, s is the spherical surface on which the concentration of oxygen is assumed to keep the initial state and c_s is a solubility limit of oxygen in the metal [2,12]. It is customarily assumed for the solubility to quickly reach at the metal–oxide interface during high temperature oxidation [12].

As mentioned in our previous paper [2], a difficulty in solving this problem is that both the metal–oxide and the oxide–oxygen (air) interfaces move with satisfying

$$\frac{\mathrm{d}R_\mathrm{i}}{\mathrm{d}t} = \frac{a\,\mathcal{D}^{(\mathrm{o})}}{c^{(\mathrm{m})}_{(\mathrm{met})}\epsilon} \left(\alpha \frac{\partial c^{(\mathrm{m})}_{(\mathrm{O}_2)}}{\partial r}\bigg|_{R_\mathrm{i}} - \frac{\partial c^{(\mathrm{o})}_{(\mathrm{O}_2)}}{\partial r}\bigg|_{R_\mathrm{i}} \right) \tag{17}$$

$$\frac{\mathrm{d}R_\mathrm{o}}{\mathrm{d}t} = \frac{\mathcal{D}^{(\mathrm{o})}(a - b\,\gamma)}{c^{(\mathrm{m})}_{(\mathrm{met})}\epsilon} \left(\frac{R_\mathrm{i}}{R_\mathrm{o}} \right)^2 \left(\alpha \frac{\partial c^{(\mathrm{m})}_{(\mathrm{O}_2)}}{\partial r}\bigg|_{R_\mathrm{i}} - \frac{\partial c^{(\mathrm{o})}_{(\mathrm{O}_2)}}{\partial r}\bigg|_{R_\mathrm{i}} \right) \tag{18}$$

These are obtained using Eq. (7) and the jump momentum balances for both interfaces. Since the metal–oxide interface is initially located at the free surface R_ini, the initial condition is

$$\text{at } t = 0: \; R_\mathrm{i}(t) = R_\mathrm{o}(t) = R_\mathrm{ini} \tag{19}$$

For simplicity, let us introduce the following dimensionless variables

$$c^{(\mathrm{m})\star} \equiv \frac{c^{(\mathrm{m})}_{(\mathrm{O}_2)}}{c_\mathrm{eq}}, \quad c^{(\mathrm{o})\star} \equiv \frac{c^{(\mathrm{o})}_{(\mathrm{O}_2)}}{c_\mathrm{eq}}, \quad t^\star \equiv t\frac{\mathcal{D}^{(\mathrm{o})}}{R^2_\mathrm{ini}}, \quad k^\star = k\frac{R_\mathrm{ini}}{\mathcal{D}^{(\mathrm{o})}}, \quad r^\star \equiv \frac{r}{R_\mathrm{ini}}, \quad R^\star_\mathrm{i} \equiv \frac{R_\mathrm{i}}{R_\mathrm{ini}}, \quad R^\star_\mathrm{o} \equiv \frac{R_\mathrm{o}}{R_\mathrm{ini}}, \quad s^\star \equiv \frac{s}{R_\mathrm{ini}} \tag{20}$$

In terms of these, Eqs. (9)–(16) are expressed as

$$\frac{1}{\alpha}\frac{\partial c^{(\mathrm{m})\star}}{\partial t^\star} - \frac{2}{r^\star}\frac{\partial c^{(\mathrm{m})\star}}{\partial r^\star} - \frac{\partial^2 c^{(\mathrm{m})\star}}{\partial r^{\star 2}} = 0 \tag{21}$$

$$\frac{\partial c^{(\mathrm{o})\star}}{\partial t^\star} - \left\{ \frac{2}{r^\star} - \frac{(a - b\gamma)c_\mathrm{eq}}{\epsilon c^{(\mathrm{m})}_{(\mathrm{met})}} \left(\frac{R^\star_\mathrm{i}}{r^\star} \right)^2 \left[\alpha \frac{\partial c^{(\mathrm{m})\star}}{\partial r^\star}\bigg|_{R^\star_\mathrm{i}} - \frac{\partial c^{(\mathrm{o})\star}}{\partial r^\star}\bigg|_{R^\star_\mathrm{i}} \right] \right\} \frac{\partial c^{(\mathrm{o})\star}}{\partial r^\star} - \frac{\partial^2 c^{(\mathrm{o})\star}}{\partial r^{\star 2}} = 0 \tag{22}$$

and

$$\text{at } t^\star = 0: \; c^{(\mathrm{m})\star} = 0 \tag{23}$$

$$\text{at } r^\star = s^\star: \; c^{(\mathrm{m})\star} = 0 \tag{24}$$

$$\text{at } r^\star = R^\star_\mathrm{i}: \; c^{(\mathrm{m})\star} = c^\star_\mathrm{s} \tag{25}$$

$$\text{at } r^\star = R^\star_\mathrm{i}: \; \frac{\partial c^{(\mathrm{o})\star}}{\partial r^\star} - \alpha \frac{\partial c^{(\mathrm{m})\star}}{\partial r^\star} = k^\star \epsilon\, c^{(\mathrm{o})\star} \tag{26}$$

$$\text{at } r^\star = R^\star_\mathrm{o}: \; c^{(\mathrm{o})\star} = 1 \tag{27}$$

Eqs. (17) through (19) become

$$\frac{\mathrm{d}R^\star_\mathrm{i}}{\mathrm{d}t^\star} = \frac{a}{\epsilon}\frac{c_\mathrm{eq}}{c^{(\mathrm{m})}_{(\mathrm{met})}} \left(\alpha \frac{\partial c^{(\mathrm{m})\star}}{\partial r^\star}\bigg|_{R^\star_\mathrm{i}} - \frac{\partial c^{(\mathrm{o})\star}}{\partial r^\star}\bigg|_{R^\star_\mathrm{i}} \right) \tag{28}$$

$$\frac{\mathrm{d}R^\star_\mathrm{o}}{\mathrm{d}t^\star} = \frac{a - b\,\gamma}{\epsilon}\frac{c_\mathrm{eq}}{c^{(\mathrm{m})}_{(\mathrm{met})}} \left(\frac{R^\star_\mathrm{i}}{R^\star_\mathrm{o}} \right)^2 \left(\alpha \frac{\partial c^{(\mathrm{m})\star}}{\partial r^\star}\bigg|_{R^\star_\mathrm{i}} - \frac{\partial c^{(\mathrm{o})\star}}{\partial r^\star}\bigg|_{R^\star_\mathrm{i}} \right) \tag{29}$$

and

$$\text{at } t^\star = 0: \; R_\mathrm{i}^\star = R_\mathrm{o}^\star = 1 \tag{30}$$

Now, we introduce two Landau transformations in order to transform both of the moving interfaces into a fixed domain:

$$\chi \equiv \frac{r^\star}{R_\mathrm{i}^\star} \tag{31}$$

and

$$\zeta \equiv \frac{\chi - 1}{\chi_\mathrm{o} - 1} \tag{32}$$

where $\chi_\mathrm{o} = R_\mathrm{o}^\star / R_\mathrm{i}^\star$. By the chain rule to transform from $c^\star(r^\star, t^\star)$ to $c^\star(\zeta, \chi_\mathrm{o})$, Eqs. (21)–(27) can be written as

$$\frac{\phi}{\alpha\epsilon}\left(\alpha\frac{\partial c^{(\mathrm{m})\star}}{\partial\zeta}\bigg|_{\zeta=0} - \frac{\partial c^{(\mathrm{o})\star}}{\partial\zeta}\bigg|_{\zeta=0}\right)\left\{\left(\frac{a-b\gamma}{\chi_\mathrm{o}^2} - a\chi_\mathrm{o}\right)\left[(\chi_\mathrm{o}-1)\frac{\partial c^{(\mathrm{m})\star}}{\partial\chi_\mathrm{o}} - \zeta\frac{\partial c^{(\mathrm{m})\star}}{\partial\zeta}\right] - a(\zeta\chi_\mathrm{o} - \zeta + 1)\frac{\partial c^{(\mathrm{m})\star}}{\partial\zeta}\right\}$$
$$= \frac{2(\chi_\mathrm{o}-1)}{\zeta\chi_\mathrm{o} - \zeta + 1}\frac{\partial c^{(\mathrm{m})\star}}{\partial\zeta} + \frac{\partial^2 c^{(\mathrm{m})\star}}{\partial\zeta^2} \tag{33}$$

$$\frac{\phi}{\epsilon}\left(\alpha\frac{\partial c^{(\mathrm{m})\star}}{\partial\zeta}\bigg|_{\zeta=0} - \frac{\partial c^{(\mathrm{o})\star}}{\partial\zeta}\bigg|_{\zeta=0}\right)\left\{\left(\frac{a-b\gamma}{\chi_\mathrm{o}^2} - a\chi_\mathrm{o}\right)\left[(\chi_\mathrm{o}-1)\frac{\partial c^{(\mathrm{o})\star}}{\partial\chi_\mathrm{o}} - \zeta\frac{\partial c^{(\mathrm{o})\star}}{\partial\zeta}\right]\right.$$
$$\left. - \left[a(\zeta\chi_\mathrm{o} - \zeta + 1) - \frac{a-b\gamma}{(\zeta\chi_\mathrm{o} - \zeta + 1)^2}\right]\frac{\partial c^{(\mathrm{o})\star}}{\partial\zeta}\right\} = \frac{2(\chi_\mathrm{o}-1)}{\zeta\chi_\mathrm{o} - \zeta + 1}\frac{\partial c^{(\mathrm{o})\star}}{\partial\zeta} + \frac{\partial^2 c^{(\mathrm{o})\star}}{\partial\zeta^2} \tag{34}$$

and

$$\text{at } \chi_\mathrm{o} = 1: \; c^{(\mathrm{m})\star} = 0 \tag{35}$$

$$\text{at } \zeta = -\delta \equiv \frac{s^\star/(R_\mathrm{i}^\star - 1)}{\chi_\mathrm{o} - 1}: \; c^{(\mathrm{m})\star} = 0 \tag{36}$$

$$\text{at } \zeta = 0: \; c^{(\mathrm{m})\star} = c_\mathrm{s}^\star \tag{37}$$

$$\text{at } \zeta = 0: \; \frac{\partial c^{(\mathrm{o})\star}}{\partial\zeta} - \alpha\frac{\partial c^{(\mathrm{m})\star}}{\partial\zeta} = k^\star R_\mathrm{i}^\star \epsilon\,(\chi_\mathrm{o} - 1)\,c^{(\mathrm{o})\star} \tag{38}$$

$$\text{at } \zeta = 1: \; c^{(\mathrm{o})\star} = 1 \tag{39}$$

Here, we have used the ratio of speed of displacements of the oxide–oxygen (air) interface to the metal–oxide interface:

$$\frac{\mathrm{d}\chi_\mathrm{o}}{\mathrm{d}t^\star} = \frac{\phi}{R_\mathrm{i}^{\star 2}\,(\chi_\mathrm{o}-1)\epsilon}\left(\frac{a-b\gamma}{\chi_\mathrm{o}^2} - a\chi_\mathrm{o}\right)\left(\alpha\frac{\partial c^{(\mathrm{m})\star}}{\partial\zeta}\bigg|_{\zeta=0} - \frac{\partial c^{(\mathrm{o})\star}}{\partial\zeta}\bigg|_{\zeta=0}\right) \tag{40}$$

and we have introduced

$$\phi \equiv \frac{c_\mathrm{eq}}{c_{(\mathrm{met})}^{(\mathrm{m})}} \tag{41}$$

Note that the relation between χ_o and $R_\mathrm{i}^\star$ can be derived by Eqs. (28)–(30). For the metal layer, Eq. (33) has to be solved with Eqs. (35) through (37). Here, δ will be assumed to be constant [2,8]. For the oxide layer, Eq. (34) has to be solved with Eqs. (38) and (39).

3.1. Perturbation analysis

Since $\phi \ll 1$ in most practical cases, a regular perturbation analysis using ϕ as a perturbation parameter can be applied for solving these equations:

$$c^{(\mathrm{m})\star}(\zeta, \chi_\mathrm{o}) = c_0^{(\mathrm{m})}(\zeta, \chi_\mathrm{o}) + \phi c_1^{(\mathrm{m})}(\zeta, \chi_\mathrm{o}) + \phi^2 c_2^{(\mathrm{m})}(\zeta, \chi_\mathrm{o}) + \cdots \tag{42}$$

$$c^{(\mathrm{o})\star}(\zeta, \chi_\mathrm{o}) = c_0^{(\mathrm{o})}(\zeta, \chi_\mathrm{o}) + \phi c_1^{(\mathrm{o})}(\zeta, \chi_\mathrm{o}) + \phi^2 c_2^{(\mathrm{o})}(\zeta, \chi_\mathrm{o}) + \cdots \tag{43}$$

These are substituted into Eqs. (33)–(39) and the terms are ordered by the powers of ϕ. The result is a sequence of systems of equations for the zeroth-order solutions $c_0^{(m)}$ and $c_0^{(o)}$, for the first-order solutions $c_1^{(m)}$ and $c_1^{(o)}$, and for the second-order solutions $c_2^{(m)}$ and $c_2^{(o)}$, etc. For a small ϕ, the first-order perturbation solutions are enough to describe the concentration of oxygen.

3.1.1. Zeroth-order perturbation

From Eqs. (33), (42), and (43), the zeroth-order equation for the metal layer is

$$\frac{2(\chi_o - 1)}{\zeta\chi_o - \zeta + 1}\frac{\partial c_0{}^{(m)}}{\partial\zeta} + \frac{\partial^2 c_0{}^{(m)}}{\partial\zeta^2} = 0 \tag{44}$$

which should be solved with the zeroth-order perturbations of Eqs. (36) and (37):

$$\text{at } \zeta = -\delta:\ c_0{}^{(m)} = 0 \tag{45}$$

$$\text{at } \zeta = 0:\ c_0^{(m)} = c_s^\star \tag{46}$$

The solution of Eq. (44) consistent with Eqs. (45) and (46) is

$$c_0^{(m)} = c_s^\star\left(\frac{\zeta + \delta}{\delta(1 - \zeta + \zeta\chi_o)}\right) \tag{47}$$

The zeroth-order equation for the oxide layer is obtained from Eqs. (34), (42), and (43)

$$\frac{2(\chi_o - 1)}{\zeta\chi_o - \zeta + 1}\frac{\partial c_0^{(o)}}{\partial\zeta} + \frac{\partial^2 c_0^{(o)}}{\partial\zeta^2} = 0 \tag{48}$$

Integrating this consistent with the zeroth-order perturbations of Eqs. (38) and (39)

$$\text{at } \zeta = 0:\ \frac{\partial c_0^{(o)}}{\partial\zeta} - \alpha\frac{\partial c_0^{(m)}}{\partial\zeta} = k^\star R_i^\star\epsilon(\chi_o - 1)c_0^{(o)} \tag{49}$$

$$\text{at } \zeta = 1:\ c_0^{(o)} = 1 \tag{50}$$

we have

$$c_0^{(o)} = \frac{\alpha c_s^\star(\zeta - 1)(1 + \delta - \delta\chi_o) + \delta\chi_o[1 + \zeta(\chi_o - 1)(1 + k^\star R_i^\star\epsilon)]}{\delta(1 - \zeta + \zeta\chi_o)[k^\star R_i^\star\epsilon(\chi_o - 1) + \chi_o]} \tag{51}$$

Note that the zeroth-order solutions (47) and (51) represent quasi-steady-state solutions which can be obtained from Eqs. (33) and (34) by discarding the time derivatives. When the oxidation is instantaneous, i.e., $k^\star \to \infty$, the oxygen concentration in the oxide Eq. (51) corresponds to the analytical solution obtained by Crank [15].

3.1.2. First-order perturbation

Looking at the coefficient of ϕ in Eq. (33) substituted by Eqs. (42) and (43), we have

$$\frac{2(\chi_o - 1)}{\zeta\chi_o - \zeta + 1}\frac{\partial c_1^{(o)}}{\partial\zeta} + \frac{\partial^2 c_1^{(o)}}{\partial\zeta^2} = \frac{1}{\alpha\epsilon}\left\{\left(\frac{a - b\gamma}{\chi_o^2} - a\,\chi_o\right)\left[(\chi_o - 1)\frac{\partial c_0^{(m)}}{\partial\chi_o} - \zeta\frac{\partial c_0^{(m)}}{\partial\zeta}\right] - a(\zeta\chi_o - \zeta + 1)\frac{\partial c_0^{(m)}}{\partial\zeta}\right\}$$
$$\times\left(\alpha\frac{\partial c_0^{(m)}}{\partial\zeta}\bigg|_{\zeta=0} - \frac{\partial c_0^{(o)}}{\partial\zeta}\bigg|_{\zeta=0}\right) \tag{52}$$

The corresponding boundary conditions are from Eqs. (36) and (37)

$$\text{at } \zeta = -\delta:\ c_1^{(m)} = 0 \tag{53}$$

$$\text{at } \zeta = 0:\ c_1^{(m)} = 0 \tag{54}$$

Substituting the zeroth-order solutions (47) and (51) into Eq. (52) and integrating twice, we can find

$$c_1^{(m)} = \frac{c_s^\star k^\star R_i^\star\zeta(\delta + \zeta)(\chi_o - 1)[c_s^\star\alpha(1 + \delta - \delta\chi_o) - \delta\chi_o]}{6\alpha\delta^2\chi_o^2(1 - \zeta + \zeta\chi_o)[k^\star R_i^\star\epsilon(\chi_o - 1) + \chi_o]} \times\left[(a - b\gamma)(\delta - \zeta) - 3a(1 + \delta)\chi_o^2 + a(2\delta + \zeta)\chi_o{}^3\right] \tag{55}$$

From Eqs. (34), (42) and (43), the first-order equation for the oxide layer is

$$\frac{2(\chi_o-1)}{\zeta\chi_o-\zeta+1}\frac{\partial c_1^{(o)}}{\partial\zeta}+\frac{\partial^2 c_1^{(o)}}{\partial\zeta^2}=\frac{1}{\epsilon}\left\{\left(\frac{a-b\gamma}{\chi_o^2}-a\chi_o\right)\left[(\chi_o-1)\frac{\partial c_0^{(o)}}{\partial\chi_o}-\zeta\frac{\partial c_0^{(o)}}{\partial\zeta}\right]\right.$$
$$\left.-\left[a(\zeta\chi_o-\zeta+1)-\frac{a-b\gamma}{(\zeta\chi_o-\zeta+1)^2}\right]\frac{\partial c_0^{(o)}}{\partial\zeta}\right\}\times\left(\alpha\frac{\partial c_0^{(m)}}{\partial\zeta}\bigg|_{\zeta=o}-\frac{\partial c_0^{(o)}}{\partial\zeta}\bigg|_{\zeta=0}\right) \tag{56}$$

This is to be solved consistent with

$$\text{at } \zeta=0:\ \frac{\partial c_1^{(o)}}{\partial\zeta}-\alpha\frac{\partial c_1^{(m)}}{\partial\zeta}=k^\star R_i^\star\epsilon(\chi_o-1)c_1^{(o)} \tag{57}$$

$$\text{at } \zeta=1:\ c_1^{(o)}=0 \tag{58}$$

Eqs. (56)–(58) are satisfied with

$$c_1^{(o)}=f(\zeta,\chi_o) \tag{59}$$

in which functions $f(\zeta, \chi_o)$ is obtained by *Mathematica*.

3.2. Oxide thickness

In order to obtain the oxide thickness, Eqs. (42) and (43) are substituted into Eq. (40) and the terms are ordered by the powers of ϕ:

$$\frac{d\chi_o}{dt^\star}=\frac{\phi}{R_i^{\star 2}(\chi_o-1)\epsilon}\left(\frac{a-b\gamma}{\chi_o^2}-a\chi_o\right)\times\left\{\alpha\frac{\partial c_0^{(m)}}{\partial\zeta}\bigg|_{\zeta=0}-\frac{\partial c_0^{(o)}}{\partial\zeta}\bigg|_{\zeta=0}+\phi\left(\alpha\frac{\partial c_1^{(m)}}{\partial\zeta}\bigg|_{\zeta=0}-\frac{\partial c_1^{(o)}}{\partial\zeta}\bigg|_{\zeta=0}\right)+\cdots\right\} \tag{60}$$

From Eqs. (28) and (29), we have

$$dR_o^{\star 3}=\left(1-\frac{b}{a}\gamma\right)dR_i^{\star 3} \tag{61}$$

In view of Eq. (30), we find

$$R_o^{\star 3}=\left(1-\frac{b}{a}\gamma\right)R_i^{\star 3}+\frac{b}{a}\gamma \tag{62}$$

Since $\chi_o=R_o^\star/R_i^\star$, $R_i^\star$ can be written as

$$R_i^\star=\left(\frac{b\gamma}{a\chi_o^3+b\gamma-a}\right)^{1/3} \tag{63}$$

Substituting Eqs. (47), (51), (55), (59) and (63) into Eq. (60), we have

$$\frac{d\chi_o}{dt^\star}=\frac{k^\star\Omega[c_s^\star\alpha(1+\delta-\delta\chi_o)-\delta\chi_o]}{\delta(\Theta+\chi_o)}\left(\phi\left[\frac{a\chi_o^3+b\gamma-a}{b\gamma}\right]^{1/3}+\phi^2\frac{k^\star(\chi_o-1)}{6b\gamma\delta\chi_o^2(\Theta+\chi_o)^3}\left\{a\left[b\gamma(\Theta+\chi_o)(-3\delta\Theta(\chi_o-1)\chi_o^2\right.\right.\right.$$
$$+c_s^\star\{3\delta[-\Theta+\alpha(\chi_o-1)^2-\chi_o]\chi_o^2-3\alpha(\chi_o-1)^2\chi_o^2+\delta^2(\chi_o-1)^2(\Theta+\chi_o)(1+2\chi_o)\})$$
$$\left.+2\frac{b\gamma}{a\chi_o^3+b\gamma-a}\Theta(\chi_o-1)\chi_o^4\Omega[c_s^\star\alpha(1+\delta-\delta\chi_o)-\delta\chi_o]\right]-b\gamma(b\gamma(\Theta+\chi_o)\{3\delta\Theta\chi_o^3+c_s^\star[3\alpha\chi_o^2-3\alpha\delta(\chi_o-1)\chi_o^2$$
$$\left.\left.+\delta^2(\Theta+\chi_o)]\}+\chi_o^2[\delta\Theta(2+\Theta+\chi_o)-c_s^\star\alpha[-2+\Theta+\chi_o+\delta(\chi_o-1)(2+\Theta+\chi_o)]]\})\right\}\right)+\cdots \tag{64}$$

where

$$\Omega\equiv\frac{a-b\gamma}{\chi_o^2}-a\chi_o,\quad \Theta\equiv k^\star\epsilon(\chi_o-1)\left(\frac{b\gamma}{a\chi_o^3}+b\gamma-a\right)^{1/3} \tag{65}$$

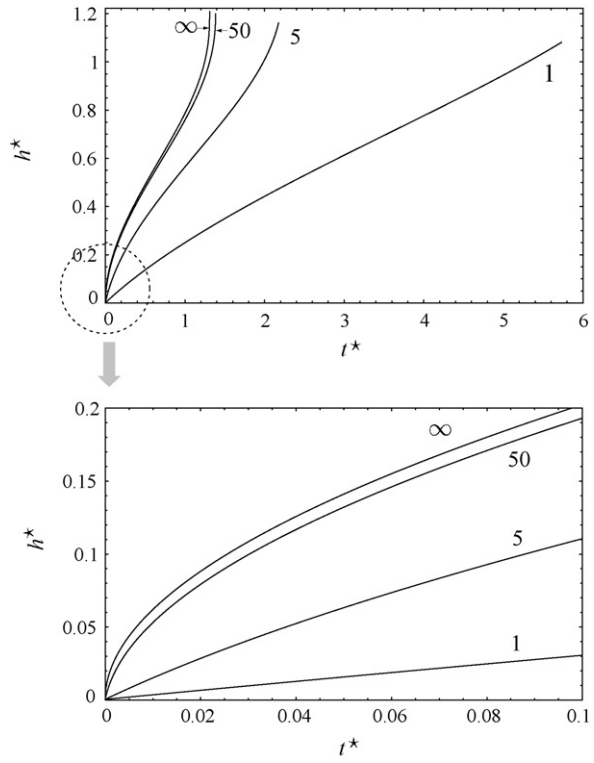

Fig. 2. Oxide thickness $h^\star (= R_o^\star - R_i^\star)$ for four different values of $k^\star$ where $k^\star = R_{ini}\, k/\mathcal{D}^{(o)}$.

Using Eqs. (62)–(64), we can get $R_i^\star$ and $R_o^\star$ as a function of time. Then we can also obtain the concentration of oxygen using Eqs. (47), (51), (55) and (59).

Now let us simplify Eq. (64) for a special case. In the case of $k^\star \to \infty$ and $a = b = \gamma = 1$ with no oxygen diffusion into the metal, Eq. (64) reduces to

$$\frac{dR_i^\star}{dt^\star} = \frac{\phi}{R_i^\star(R_i^\star - 1)}\left\{1 - \frac{\phi}{3R_i^\star} + \cdots\right\} \tag{66}$$

When $R_i^\star = R_i/R_{ini} \approx 1$ during the oxidation, i.e., the thickness of the oxide $R_{ini} - R_i$ is much thinner than that of the initial metal R_{ini}, the effect of curvature disappears and thus Eq. (66) corresponds to the result for the oxidation on a metal plane (Eq. (75) in Ref. [1]).

4. $k^\star$ Dependence on oxide thickness

Using the perturbation solution (64), we plot in Fig. 2 the oxide thickness for different values of $k^\star$. Here, we have taken $a = b = 1$, $\gamma = 1.78$, $\phi = 0.18$, $c_s^\star = 0.86$, and $\epsilon = 1.12$, which correspond to the values given by Imbrie and Lagoudas [8]. The α defined as Eq. (11) is assumed to be 0.12 [1]. Similarly, with our previous results for flat and cylindrical geometries [1,2], increase in $k^\star$ transforms the growth rate of the oxide from linear to parabolic.

In addition, the oxide growth abruptly increases at the late stage of the oxidation as $k^\star$ increases. At this stage, the radius of the remaining metal is much smaller than that at the early stage of the oxidation. This means that increase in the oxide thickness by volumetric expansion at the late stage is much higher than that at the early stage. However, the abrupt increase disappears as $k^\star$ decreases since the increase is relieved by the slow oxidation reaction.

5. Comparison to a numerical solution

Recently, the oxidation of a titanium sphere has been numerically solved by Entchev et al. [3]. The oxygen concentration in the very thin oxide layer was assumed to be linear during the early stages of oxidation. They also assumed that the reaction at the Ti–TiO_2 interface is instantaneous, and that there is no oxygen diffusion into the metal through the metal–oxide interface. In order to compare with their results, we use Eq. (64) with $a = b = 1$, $\epsilon = 1$, $c_s^\star = 0$, and $k^\star \to \infty$. We also take $\gamma = 1.77$ and $\mathcal{D}_{(O_2,TiO_2)} = 1.34 \times 10^{-3}\ \mu m^2/s$ used in their numerical analysis. As shown in Fig. 3(a), the oxide thickness predicted by the perturbation analysis is comparable to that by the numerical analysis. In Fig. 3(b), we repeated their numerical calculation for the

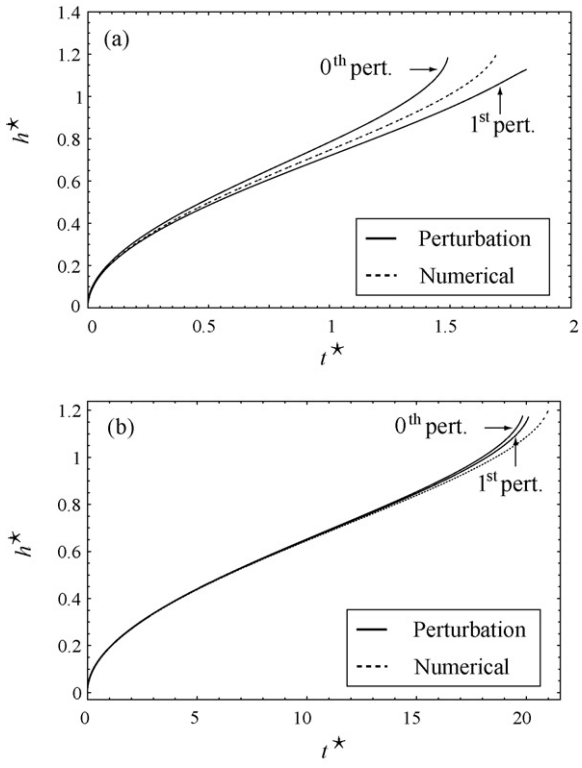

Fig. 3. Comparison of the oxide thickness predicted by the perturbation analysis to that numerically calculated by Entchev et al. [3]: (a) for a given $\phi = 0.13$ in their analysis, and (b) for an arbitrary value $\phi = 0.01$. Here, $h^\star = R_o^\star - R_i^\star$.

oxidation of $\phi = 0.01$ and showed that for such a small ϕ the zeroth-order perturbation solution in Section 3.1.1 is enough to describe the oxide thickness as well as the concentration of oxygen.

For the case of silicon oxidation, the Pilling-Bedworth ratio is 2.15 [16] and ϕ is generally of the order of 10^{-6} [17]. It is generally known that there occurs no oxygen diffusion into the silicon substrate. Thus, for the silicon oxidation, we can use Eq. (64) with $a = b = 1$, $\epsilon = 1$, $c_s^\star = 0$, and $k^\star \to \infty$. This result is displayed in Fig. 4.

6. Stress developed during the oxidation

In this section, we simply mention how to calculate the stress developed during the oxidation of the metal sphere. Typically, the density of the oxide is less than that of the metal. This results in the molecular mismatch and the volumetric expansion at the metal–oxide interface and thus stresses develop in both the metal and the oxide as oxidation proceeds. Oh et al. [4] have solved stress distributions during the oxidation of metal cylinders by an inelastic approach. In a similar way, we solve the stress developed during the oxidation of the metal sphere.

It is reasonable to assume that the oxide and the metal move in the direction of r only during the oxidation. This means that the displacements in θ and φ directions are zero, and that the displacement in r direction, u_r, is a function of r only. Using the Navier

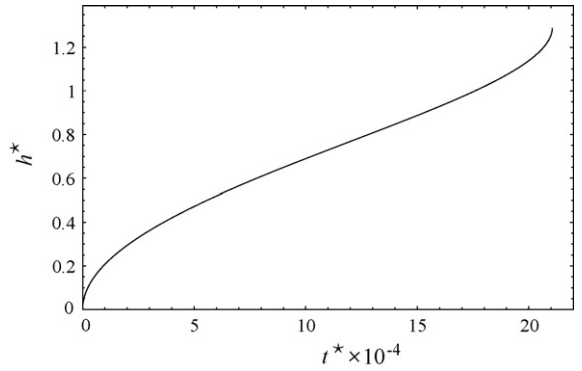

Fig. 4. The thickness of silicon oxide predicted by the perturbation analysis. Here, $h^\star = R_o^\star - R_i^\star$.

equation, Little [18] has shown

$$u_r = Ar + \frac{B}{r^2} \tag{67}$$

when no body force is applied.

In view of assumption (vii), the non-zero components of strain and stress become

$$\varepsilon_{rr} = A - \frac{2B}{r^3}, \quad \varepsilon_{\theta\theta} = \varepsilon_{\varphi\varphi} = A + \frac{B}{r^3} \tag{68}$$

and

$$\sigma_{rr} = \frac{E}{1-2\nu}A - \frac{2B}{(1+\nu)r^3}, \quad \sigma_{\theta\theta} = \sigma_{\varphi\varphi} = \frac{E}{1-2\nu}A + \frac{B}{(1+\nu)r^3}, \tag{69}$$

Eqs. (67) through (69) should be satisfied for each phase.

In order to obtain the coefficients for each phase, the following boundary conditions have to be applied:

$$\text{at } r = 0: \ \sigma_{rr}^{(\mathrm{o})} < \infty \tag{70}$$

$$\text{at } r = R_\mathrm{i}: \ \sigma_{rr}^{(\mathrm{m})} = \sigma_{rr}^{(\mathrm{o})} \tag{71}$$

$$\text{at } r = R_\mathrm{o}: \ \sigma_{rr}^{(\mathrm{o})} = 0 \tag{72}$$

$$\gamma = \frac{(R_\mathrm{o}^3 - R_\mathrm{i}^3)[1 - \mathrm{tr}(\boldsymbol{\varepsilon}^{(\mathrm{o})})]}{R_\mathrm{ini}^3 - R_\mathrm{i}^3[1 - \mathrm{tr}(\boldsymbol{\varepsilon}^{(\mathrm{m})})]} \tag{73}$$

Eqs. (71) and (72) are obtained from the jump momentum balance [14]. Eq. (73) is from the fact that the number of moles of the metal consumed by oxidation is the same as the number of moles of the oxide formed in a stress-free conditions. More details on these are described in our previous work [4].

Using (68) through (73), we conclude that

$$\begin{aligned}
\sigma_{rr}^{(\mathrm{m})} = \sigma_{\theta\theta}^{(\mathrm{m})} = \sigma_{\varphi\varphi}^{(\mathrm{m})} &= \frac{E^{(\mathrm{m})}E^{(\mathrm{o})}[R_\mathrm{o}^3 + R_\mathrm{i}^3(\gamma-1) - R_\mathrm{ini}^3\gamma]}{3R_\mathrm{i}^3[E^{(\mathrm{m})}(2\nu^{(\mathrm{o})}-1) - E^{(\mathrm{o})}\gamma(2\nu^{(\mathrm{m})}-1)]} \\
\sigma_{rr}^{(\mathrm{o})} &= \frac{E^{(\mathrm{m})}E^{(0)}[R_\mathrm{o}^3 + R_\mathrm{i}^3(\gamma-1) - R_\mathrm{ini}^3\gamma]}{3[E^{(\mathrm{m})}(2\nu^{(0)}-1) - E^{(0)}\gamma(2\nu^{(\mathrm{m})}-1)](R_\mathrm{i}^3 - R_\mathrm{o}^3)}\left(1 - \frac{R_\mathrm{o}^3}{r^3}\right) \\
\sigma_{\theta\theta}^{(\mathrm{o})} = \sigma_{\varphi\varphi}^{(\mathrm{o})} &= \frac{E^{(\mathrm{m})}E^{(0)}[R_\mathrm{o}^3 + R_\mathrm{i}^3(\gamma-1) - R_\mathrm{ini}^3\gamma]}{3[E^{(\mathrm{m})}(2\nu^{(0)}-1) - E^{(0)}\gamma(2\nu^{(\mathrm{m})}-1)](R_\mathrm{i}^3 - R_\mathrm{o}^3)}\left(1 + \frac{R_\mathrm{o}^3}{2r^3}\right)
\end{aligned} \tag{74}$$

Here, R_i and R_o are functions of time and calculated from the solution to the oxidation problem in Section 3.

7. Conclusions

The perturbation analysis was successfully applied to model the one-dimensional oxidation of a metal sphere. It should be noted that the following typical assumptions employed in literature [11,12,7,3] have not been used; no oxygen diffusion into metal, no volumetric expansion, a diffusion-controlled reaction. The perturbation results for the oxidation of the titanium sphere were well-fitted to the numerical ones calculated by Entchev et al. [3].

The inelastic approach first employed for cylindrical systems [4] was extended to calculate the stress distribution developed during the oxidation of the metal sphere. The stresses were expressed as both the Pilling-Bedworth ratio and the moving interfaces which can be determined from either the perturbation analysis or experiments.

References

[1] E.-S. Oh, A diffusional analysis for the oxidation on a plane metal–oxide interface, Chem. Eng. J. 117 (2006) 143–154.
[2] E.-S. Oh, A perturbation analysis for the metal oxidation fo cylindrical geometries, J. Chem. Eng. Japan 39 (1) (2006) 57–67.
[3] P.B. Entchev, D.C. Lagoudas, J.C. Slattery, Effects of non-planar geometries and volumetric expansion in the modeling of oxidation in titanium, Int. J. Eng. Sci. 39 (2001) 695–714.
[4] E.-S. Oh, J.R. Walton, D.C. Lagoudas, J.C. Slattery, Evolution of stresses in a simple class of oxidation problems, Acta Mechanica 181 (2006) 231–255.
[5] D. Kao, J.P. Mcvittie, W.D. Nix, K.C. Saraswat, Two-dimensional thermal oxidation of silicon-I, Experiments, IEEE Trans. Elec. Dev. 34 (5) (1987) 1008–1017.
[6] D. Kao, M. Manley, C. Blair, G. Scott, H.W.M. Chung, K. Brown, N. Narahari, E.R. Myers, C.-M. Shyu, Two-dimensional effects in titanium silicidation, IEEE Trans. Elec. Dev. 45 (1) (1998) 187–192.
[7] D.C. Lagoudas, X. Ma, D.A. Miller, D.H. Allen, Modeling of oxidation in metal matrix composites, Int. J. Eng. Sci. 33 (15) (1995) 2327–2343.

[8] P.K. Imbrie, D.C. Lagoudas, The morphological evolution of TiO_2 scale formed on various 1-d and 2-d geometries of titanium, Oxid. Met. 55 (3–4) (2001) 359–399.
[9] R. Karmhag, G.A. Niklasson, M. Nygren, Oxidation kinetics of small nickel particles, J. Appl. Phys. 85 (2) (1999) 1186–1191.
[10] T. Liu, H. Shao, X. Li, Oxidation behavior of Fe_3Al nanoparticles prepared by hydrogen plasma–metal reaction, Nanotechnology 14 (2003) 542–545.
[11] R.E. Carter, Kinetic model for solid-state reactions, J. Chem. Phys. 34 (6) (1961) 2010–2015.
[12] J. Unnam, R.N. Shenoy, R.K. Clark, Oxidation of commercial purity titanium, Oxid. Met. 26 (3) (1986) 231–252.
[13] H.G. Landau, Heat conduction in a melting solid, Q. Appl. Math. 8 (1950) 81–94.
[14] J.C. Slattery, Advanced Transport Phenomena, 1st ed., Cambridge University Press, Cambridge, 1999.
[15] J. Crank, The Mathematics of Diffusion, Clarendon Press, Oxford, 1975.
[16] H.E. Evans, Stress effects in high temperature oxidation of metals, Int. Mater. Rev. 40 (1) (1995) 1–39.
[17] V.R. Mhetar, L.A. Archer, A perturbation solution for the interfacial oxidation of silicon, J. Vac. Sci. Technol. B 16 (4) (1998) 2121–2124.
[18] R.W. Little, Elasticity, Dover Publications Inc., New York, 1999.